Available online at www.sciencedirect.com
ScienceDirect
Journal of Sound and Vibration 298 (2006) 393–403
JOURNAL OF SOUND AND VIBRATION
www.elsevier.com/locate/jsvi

An admittance function of active piezoelectric elements bonded on a cracked beam

You-Di Kuang, Guo-Qing Li*, Chuan-Yao Chen

School of Civil Engineering and Mechanics, Huazhong University of Science and Technology, Wuhan 430074, Hubei, PR China

Received 25 May 2005; received in revised form 6 April 2006; accepted 29 May 2006
Available online 7 August 2006

Abstract

The electric admittance function of the piezoelectric patches bonded on a beam with an open crack is presented, for the purpose of theoretically evaluating the health conditions of the cracked beam. At first, a sandwich beam with two layers of piezoelectric actuators is regarded as a piezoelectric bimorph, and the dynamics of the bimorph is represented by a 5×5 piezoelectric impedance matrix. Secondly, the dynamics of the elastic beam is also represented by a 4×4 impedance matrix, which is a degenerative form of piezoelectric impedance. Thirdly, the open crack is modeled as rotational massless spring and an expression of the equivalent stiffness is adopted, then the spring is used to connect the adjacent elastic beam segments. Furthermore, the cracked beam is represented by three elastic beam segments and one piezoelectric bimorph segment together with one spring. The admittance function of the piezoelectric elements is obtained by solving the linear impedance equations considering the mechanical–electric boundary conditions and the continuum conditions between the beam segments and the spring. Lastly, the effects of the crack depth and location on the admittance are examined in two numeric examples. It is found that the frequency changes and the admittance amplitude changes of the beam due to the crack can be predicted by the piezoelectric admittance function, and the modal frequencies calculated by the proposed method are accord with the results obtained by experiments and other methods. The possible application of the admittance function to detect the crack on the beam is discussed at the end of the paper as well.

1. Introduction

Cracks present a serious threat to the performance of structures and maybe will cause the catastrophic sequent. Therefore, the dynamics of cracked structures was considered as a very important topic in history. Because of the developments of smart materials and structures and the relevant research on applications of piezoelectric materials to structural health monitoring, the cracked beams with piezoelectric sensors and/or actuators are of many researcher's interest and are treated as basic problems involved in the scientific fields mentioned above.

In the past years, lots of research work about the damaged beam has been done. In some researches the presence of a crack and the corresponding reduction of the flexural beam stiffness have been represented by

*Corresponding author. Tel.: +86 27 87541715; fax: +86 27 87543501.
E-mail address: lig57@mail.hust.edu.cn (G.-Q. Li).

0022-460X/$ - see front matter
doi:10.1016/j.jsv.2006.05.032

Nomenclature

p	subscript, represents the piezoelectric layer in piezoelectric bimorph
e	subscript, represents the elastic layer in piezoelectric bimorph or the elastic beam
b	subscript, represents the piezoelectric bimorph
ρ_e, ρ_p	the mass density
$\bar{\rho}_b$	the mass of per unit length of piezoelectric bimorph
v	Poisson's ratio
S_{e11}, S_{p11}^{E}	the axial compliance modulus of elastic layer and the piezoelectric layer
d_{31}, u_{33}^{σ}	the piezoelectric strain constant and the dielectric permittivity in constant stress condition
E_3, D_3	the applied electric field and the electric displacement along the z axial direction
w, ϕ	the lateral displacement and rotational displacement
M, Q	the transverse bending moment and shear force
t, ω	the temporal variable and the electric working frequency
I, V	the electric current and voltage on piezoelectric actuator
w_p, l_p, h_p	the width, length and thickness of piezoelectric layer in bimorph
E_e, E_p	the elastic modulus of the elastic beam and the piezoelectric actuators
w_e, h_e	the thickness of elastic layer in bimorph or the thickness of the elastic beam
Y	the measured electrical admittance
k	the wave number of the piezoelectric actuator
A	the area of electric rod
a	the depth of single-edge crack
η	the loss factor of the materials

means of linear spring [1], whose stiffness may be related to the crack depth by the linear elastic fracture mechanics theory. Ju et al. [2] had theoretically related the magnitude of the equivalent linear spring constants to the length of the crack in the beam based on LEFM. This kind of model had successfully applied to simply supported [3,4] cantilever [5] and free–free [6] cracked beams. Christides and Barr [7] and Shen and Pierre [8] used either a two-term Rayleigh–Ritz [7] or the Galerkin method [8] to evaluate the influence of crack parameters on the dynamic characteristic of beam. In the above two approaches, a crack function representing the perturbation in stress field induced by the crack was considered. Fernandez-Saez et al. [9] provided a closed-form expression for the simply supported cracked beam. A variational approach to the problem of cracked beams had been used by Chondros et al. [10], and they developed a continuous cracked beam vibration theory for the lateral vibration of cracked Bernoulli–Euler beams with single-edge or double-edge open crack. Several authors also studied the nonlinear characteristic of open–closed crack. Chati et al. [11] studied the nonlinear case of open–closed cracks by the finite element method, and they introduced a bilinear frequency for cracked beam. Tsyfansky and Beresnevick [12] analyzed the essential nonlinear properties of open–closed cracks as a way to detect the presence of the crack. Chondros et al. [13] analyzed the changes in transverse vibration of a simply supported beam with breathing crack, experimental results are used for comparison with the analytical results.

Recently, the problems of undamaged or damaged structures with piezoelectric actuators and/or sensors are the focus of research fields of smart materials and structures and structural health monitoring. Several approaches are used to describe the dynamics of the beam with piezoelectric actuators or sensors. In the static approach [14] Crawley and Deluis used a statically determined equivalent force or moment as the amplitude of the forcing function to determine the dynamic response due to the activation of integrated induced strain actuators. Agnes [15] discussed the use of piezoelectric materials simultaneously as passive single-mode devices and active broadband actuators to suppress structural vibration, and he developed a simple modal model that predicted this behavior. Liang et al. [16,17] firstly proposed impedance method for smart beam and plate. The dynamic equilibrium at the connection between the elastic and piezoelectric elements is formulated. Cho et al. [17] presented a five-port equivalent electric circuit of piezoelectric bimorph to describe its dynamic characteristic.

In the aspect of the structural health monitoring using active piezoelectric materials, the impedance technique is often used to detect the damages in structures. Assuming that an active piezoelectric patch is attached on an uncracked beam and drives the beam to vibrate, the electromechanical impedance of the piezoelectric element is defined as the ratio of the electrical current passing the piezoelectric element to the applied AC voltage, which is expressed by [16]

$$Y = \frac{\mathrm{i}\omega A}{l_p}\left\{\left(u_{33}^{\sigma} - d_{31}^2/S_{p11}^E\right) + \frac{d_{31}^2 \tan kl_p}{S_{p11}^E kl_p}\left[\frac{Z_s}{Z_s + Z_a}\right]\right\}, \tag{1}$$

where Z_s is the driving point mechanical impedance of the beam, and Z_a the mechanical impedance of the piezoelectric element. When damages are presented in the beam, Z_s will change which will cause the change of the measured electrical admittance Y. Based on the above principle of the impedance technique, the health condition of damaged structures can be evaluated. Castanien and Liang [18] used the impedance technique and a signal processing technique called Baseline Normalized Standard Deviation to identify the damages in the aircraft fuselage structures. Lopes et al. [19] presented a non-modal-based technique to detect, locate and characterize structural damage by combining the impedance-based structural health monitoring technique with an artificial neural network. Park et al. [20] examined the feasibility of using an impedance-based health monitoring technique in monitoring a critical civil facility. Gao et al. [21,22] measured the admittance of piezoelectric patches attached on the cracked beam using the electron device named impedance analyzer. The health condition of cracked beam was evaluated using the admittance amplitude changes [21] and the crack was identified using the extracted frequencies from the measured admittance curves [22]. Naidu and Soh [23] combined the impedance technique and the FEM model to identify the location and the severity of the damage. The frequency drifts caused by the damage are also obtained from the measured admittance. Also, in health monitoring some researchers already pointed out that the crack may be identified according to the obtained frequencies date in beams [24,25].

From the above statements, it can be seen that the piezoelectric admittance is usually measured by impedance analyzer, and the modal frequencies are extracted from the measured admittance curves if the modal parameters are used in health monitoring. However, the theoretical relations between the location and depth of the crack and the piezoelectric admittance are studied by few researchers at present, or even in the simple cracked beam with active piezoelectric element.

The purpose of this paper is to build the piezoelectric admittance function of open-cracked Bernoulli–Euler beam. A cracked beam with a pair of piezoelectric patches will be well modeled using impedance matrices. In the model, the piezolaminated segment will be treated as a bimorph, and the open crack is modeled as linear spring. The piezoelectric admittance function is obtained by solving the impedance equations. Then, the effect of the crack on the admittance amplitude and modal frequencies of system may be examined in detail. Two numerical examples are used to verify the present model. Some discussions and conclusions will be given at the end of this paper.

2. Impedance matrix of piezoelectric bimorph

Herein let us consider a piezoelectric bimorph beam shown in Fig. 1, in which the material and geometric dimensions of the two thin piezoelectric layers are identical to each other, but they have opposite polling directions. Considering the bending vibration of the bimorph and neglecting the effect of shear field and rotatory inertia, the motion equation of the bimorph is given as [17]

$$\overline{K}_b \frac{\partial^4 w_b}{\partial^4 x} + \overline{\rho}_b \frac{\partial^2 w_b}{\partial^2 x} = 0, \tag{2}$$

where

$$\overline{K}_b = \frac{2}{3}\left[\frac{w_p}{S_{p11}^E}\left((h_p + h_e/2)^3 - (h_e)^3\right) + \frac{w_e}{S_{e11}}\left(h_e/2\right)^3\right], \quad \overline{\rho}_b = 2\left(w_p\rho_p h_p + w_e\rho_e h_e/2\right). \tag{3}$$

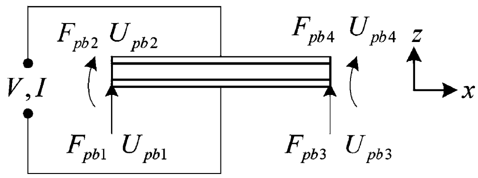

Fig. 1. The piezoelectric bimorph.

By means of the separation of variables, the general solution of the displacement in Eq. (2) can be expressed as

$$w_b = (A\cos(\lambda_b x) + B\sin(\lambda_b x) + C\cosh(\lambda_b x) + D\sinh(\lambda_b x))\mathrm{e}^{\mathrm{i}\omega t}, \tag{4}$$

where $\lambda_b^4 = \overline{\rho}_b/(\overline{K}_b)\omega^2$, A, B, C and D are the coefficients which can be determined from the boundary conditions of the bimorph.

According to the analogy theory between the electric systems and the mechanical systems, the mechanical velocities are analogy to electric flows (so that it can be called as *mechanical flows*) while the mechanical forces are analogy to be electric efforts (*mechanical efforts*). Therefore, the mechanical flows and efforts of the piezoelectric bimorph can be defined by the edge velocities and forces of piezoelectric bimorph, whose sign conventions are shown in Fig. 1:

$$\begin{aligned}
&U_{b1} = \left.\frac{\partial w_b}{\partial t}\right|_{x=0}, \quad U_{b2} = \left.\frac{\partial \phi_b}{\partial t}\right|_{x=0},\\
&U_{b3} = \left.\frac{\partial w_b}{\partial t}\right|_{x=l_p}, \quad U_{b4} = \left.\frac{\partial \phi_b}{\partial t}\right|_{x=l_p},\\
&F_{b1} = Q_b\big|_{x=0}, \quad F_{b2} = M_b|_{x=0},\\
&F_{b3} = -Q_b\big|_{x=l_p}, \quad F_{pb4} = -M_b|_{x=l_p},
\end{aligned} \tag{5}$$

where

$$M_b = \overline{K}_b\frac{\partial^2 w_b}{\partial x^2} + NV, \quad Q_b = \overline{K}_b\frac{\partial^3 w_b}{\partial x^3}, \tag{6}$$

where

$$N = -\frac{d_{31}}{s_{p11}^E} w_p\left(\frac{h_p + h_e}{2}\right).$$

The electric current passing through the piezoelectric patch actuator may be expressed as

$$I = \int_A \dot{D}_3\,\mathrm{d}A = -N(U_2 - U_4) + \mathrm{i}\omega C_c V, \tag{7}$$

where

$$A = w_p l_p, \quad C_c = \mu_{33}^\sigma\left(1 - \frac{d_{31}^2}{s_{p11}^E\mu_{33}^\sigma}\right)\frac{l_p w_p}{2h_p}.$$

Then the impedance equation for the piezoelectric bimorph beam shown in Fig. 1 can be written as

$$\mathbf{F} = \mathbf{Z}_b\mathbf{U}, \tag{8}$$

where $\mathbf{U} = \{U_{b1}, U_{b2}, U_{b3}, U_{b4}, V\}^{\mathrm{T}}$, $\mathbf{F} = \{F_{b1}, F_{b2}, F_{b3}, F_{b4}, I\}^{\mathrm{T}}$, $\mathbf{Z}_b$ is 5×5 impedance matrix, whose non-zero elements are listed as follows:

$$\begin{aligned} &Z_{11} = Z_{33} = \frac{\overline{K}_b \lambda_b^3}{\mathrm{i}\omega} \frac{-cn - sm}{1 - cm}, \quad Z_{12} = -Z_{34} = \frac{\overline{K}_b \lambda_b^2}{\mathrm{i}\omega} \frac{sn}{1 - cm}, \\ &Z_{13} = \frac{\overline{K}_b \lambda_b^3}{\mathrm{i}\omega} \frac{s + n}{1 - cm}, \quad Z_{14} = -Z_{23} = \frac{\overline{K}_b \lambda_b^2}{\mathrm{i}\omega} \frac{-c + m}{1 - cm}, \\ &Z_{22} = Z_{44} = \frac{\overline{K}_b \lambda_b}{\mathrm{i}\omega} \frac{cn - sm}{1 - cm} + \frac{N^2}{\mathrm{i}\omega C_c}, \quad Z_{24} = \frac{\overline{K}_b \lambda_b}{\mathrm{i}\omega} \frac{s - n}{1 - cm} - \frac{N^2}{\mathrm{i}\omega C_c}, \\ &Z_{25} = -Z_{45} = \frac{N}{\mathrm{i}\omega C_c}, \quad Z_{55} = \frac{1}{\mathrm{i}\omega C_c}, \end{aligned} \tag{9}$$

where

$$c = \cos(\lambda_b l_p), \quad s = \sin(\lambda_b l_p), \quad m = \cosh(\lambda_b l_p), \quad n = \sinh(\lambda_b l_p).$$

The detailed procedure obtaining the impedance matrix $\mathbf{Z}_b$ may refer to Ref. [17].

Because there is no electric–mechanical coupling in elastic beam, the impedance matrix $\mathbf{Z}_e$ can be obtained by setting $N = 0$ and changing the mass and rigidity of bimorph into that of elastic beam. The $\mathbf{Z}_e$ is a 4×4 impedance matrix which represents the dynamics of the elastic beam.

3. The electric admittance function of active piezoelectric elements

Two layered piezoelectric patches as active elements are bonded on a cracked beam symmetrically (see Fig. 2). The electric admittance of piezoelectric elements is measured using the impedance analyzer. The whole beam system is divided into four segments from the two ends of the piezoelectric elements and the location of the crack. Therefore, there are three elastic segments whose length are L_1, L_2, L_3, respectively, and one bimorph segment whose length is L_p. Obviously, $(L_1 + L_p + L_2 + L_3)$ is equal to the beam length L. The serial numbers of the four segments are labeled in Fig. 2 and assumed to be (n) $(n = 1,2,3,4)$ in order.

Firstly, the impedance equations of the four segments can be expressed as follows:

$$F_b^{(n)} = Z_b^{(n)} U_b^{(n)}, \ (n = 2) \tag{10}$$

for one bimorph segment, and

$$F_e^{(n)} = Z_e^{(n)} U_e^{(n)}, \ (n = 1, 3, 4) \tag{11}$$

for three elastic segments.

Next, the continuous conditions at the interface of the elastic segment (1) and the bimorph segment (2) should be considered. These conditions are given by

$$\begin{aligned} F_{e3}^{(1)} = -F_{b1}^{(2)}, \quad F_{e4}^{(1)} = -F_{b2}^{(2)}, \\ U_{e3}^{(1)} = U_{b1}^{(2)}, \quad U_{e4}^{(1)} = U_{b2}^{(2)}. \end{aligned} \tag{12}$$

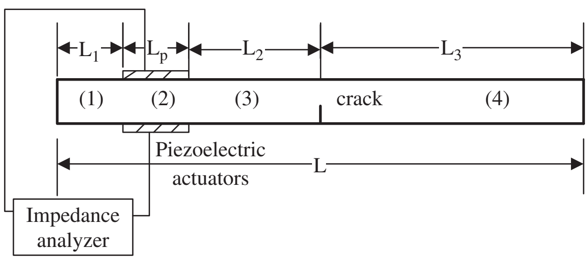

Fig. 2. The electric admittance measurement of the cracked beam.

The above continuous conditions are also adaptive to the interface between segment (2) and segment (3). It should be noticed that there are totally eight equations, which can be obtained from two equations in the same form as Eq. (12).

Thirdly, the compatible conditions in the vicinity of crack are considered. In this paper, a pair of piezoelectric patches is assumed to produce pure bending moment to the cracked elastic beam. Therefore, the equivalent stiffness of the rotational spring can be given as [26]

$$K_{\tau 1} = 1/c_1, \tag{13}$$

where

$$\begin{aligned} c_1 &= \frac{5.346 h_e}{E_e I_e} J_1\left(\frac{a}{h_e}\right), \\ J_1\left(\frac{a}{h_e}\right) &= 1.8624\left(\frac{a}{h_e}\right)^2 - 3.95\left(\frac{a}{h_e}\right)^3 + 16.375\left(\frac{a}{h_e}\right)^4 - 37.226\left(\frac{a}{h_e}\right)^5 + 76.81\left(\frac{a}{h_e}\right)^6 \\ &\quad - 126.9\left(\frac{a}{h_e}\right)^7 + 172\left(\frac{a}{h_e}\right)^8 - 43.97\left(\frac{a}{h_e}\right)^9 + 66.56\left(\frac{a}{h_e}\right)^{10} \end{aligned} \tag{14}$$

for single-edge crack, and

$$K_{\tau 2} = 1/c_2, \tag{15}$$

where

$$\begin{aligned} c_1 &= \frac{1.8495(1-\mu^2) h_e}{E_e I_e} J_1\left(\frac{2a}{h_e}\right), \\ J_2\left(\frac{2a}{h_e}\right) &= 0.63854\left(\frac{2a}{h_e}\right)^2 - 1.0385\left(\frac{2a}{h_e}\right)^3 + 3.720154\left(\frac{2a}{h_e}\right)^4 - 5.177438\left(\frac{2a}{h_{eb}}\right)^5 \\ &\quad + 7.55301\left(\frac{2a}{h_e}\right)^6 - 7.33244\left(\frac{2a}{h_e}\right)^7 + 2.49091\left(\frac{2a}{h_e}\right)^8 - 2.3391\left(\frac{2a}{h_e}\right)^9 \\ &\quad + 2.55976\left(\frac{2a}{h_e}\right)^{10} - 9.7367\left(\frac{2a}{h_e}\right)^{11} + 6.93063\left(\frac{2a}{h_e}\right)^{12} + 5.42308\left(\frac{2a}{h_e}\right)^{16} \end{aligned} \tag{16}$$

for double-edges crack [10].

In addition, the additional rotation θ^* due to the crack [10] is

$$\theta^* = \frac{E_e I_e}{K_\tau} \frac{\partial^2 w_e}{\partial x^2}, \ (K_\tau = K_{\tau 1} \ \ or \ \ K_{\tau 2}). \tag{17}$$

Then, the following relation between the left segment (3) and the right segment (4) of the crack exists:

$$\frac{\partial \theta^*}{\partial t} = \frac{E_e I_e}{K_\tau} \frac{\partial^3 w_e}{\partial x^2 \partial t} = \frac{\mathrm{i}\omega}{K_\tau} F_{e2}^{(4)} = U_{e2}^{(4)} - U_{e4}^{(3)}, \tag{18}$$

Therefore, the compatible conditions between the two segments near by the crack are

$$\begin{aligned} &U_{e3}^{(3)} = U_{e1}^{(4)}, U_{e4}^{(3)} + \mathrm{i}\omega \frac{1}{K_\tau} F_{e2}^{(4)} = U_{e2}^{(4)}, \\ &F_{e3}^{(3)} = -F_{e1}^{(4)}, \quad F_{e4}^{(3)} = -F_{e2}^{(4)}. \end{aligned} \tag{19}$$

Thirdly, the boundary conditions of the system should be considered. Assuming the driven voltage V_{in} is given, the electrical boundary conditions on the bimorph can be written as

$$V = V_{\text{in}}. \tag{20}$$

As far as the mechanical boundary conditions are concerned, three different types of mechanical boundary conditions at the two ends of the beam will be considered,

$$\begin{aligned} &\text{Free} - \text{Free ends} && F_{e1}^{(1)} = F_{e1}^{(2)} = F_{e3}^{(4)} = F_{e4}^{(4)} = 0, \\ &\text{Hinged} - \text{hinged ends} && U_{e2}^{(1)} = U_{e4}^{(4)} = 0, F_{e2}^{(1)} = F_{e4}^{(4)} = 0, \\ &\text{Clamped} - \text{free ends} && U_{e1}^{(1)} = U_{e2}^{(1)} = 0, F_{e3}^{(4)} = F_{e4}^{(4)} = 0. \end{aligned} \tag{21}$$

There are totally 34 unknown variables in Eqs. (10) and (11), and there are also 34 equations, which can be derived from Eqs. (10)–(12), (19)–(21), so that electro-mechanical field parameters in the beam system can be finally obtained by solving these linear equations.

Once the electric flow I is obtained, the electric admittance of the system will be expressed by

$$Y = I/V_{\text{in}}. \tag{22}$$

Obviously, the admittance Y is the function of the crack depth, the crack location and the other system parameters. As the admittance tends to infinity, the resonant phenomenon will happen in the system. The corresponding frequencies are the resonant frequencies of the cracked beam system. Using the impedance analyzer, the electric admittance of such system can be measured conveniently and the resonant frequencies of the cracked beam system can be extracted out [22,23]. This means that the crack in the beam can be detected using the active piezoelectric elements.

4. Numeric examples and discussions

A free–free beam with a single-edge crack will be taken as the first examples in this section, which were previously studied in the experiments by Gao et al. [21,22]. The effect of crack depth on the electric admittance of piezoelectric actuators and the frequencies will be investigated in this example. The material properties, dimensions and the relative locations of the piezoelectric actuators to the crack of the beam [21,22] are as follows:

$$\rho_e = 2700\,\text{kg/m}^3,\ Y_e = 7.1\times10^{10}\,\text{N/m}^2,\ L = 0.8\,\text{m},\ h_e = 0.008\,\text{m},\ w_e = 0.008\,\text{m},\ \eta_e = 0.006;$$
$$\rho_p = 7800\,\text{kg/m}^3,\ Y_p = 5.803\times10^{10}\,\text{N/m}^2,\ d_{31} = -1.66\times10^{-14}\,\text{m/V},\ u_{33}^{\sigma} = 1.5\times10^{-8}\,\text{F/m},\ \eta_p = 0.001;$$
$$h_p = 0.0005\,\text{m},\ w_p = 0.005\,\text{mm},\ .L_1 = 0.2\,\text{m},\ L_p = 0.025\,\text{m},\ L_2 = 0.075\,\text{m}.$$

In our theoretical calculation, the damping is considered using the loss factor η of the materials.

The admittance responses of the actuators for different crack depth ratio a/h_e are calculated and shown in Fig. 3, and the resonant frequencies of the second to the seventh mode read from Fig. 3 are also listed in Table 1. The experimental results [22] are also shown in Table 1 for comparison. It can be seen from Fig. 3 that when the crack depth ratio increases, the resonant frequencies will decrease and the peak values of the admittance at the resonant frequencies points will decrease as well. These phenomena have been observed in the experiments by Gao et al. [21] and their measured curves are also referenced in Fig. 4 for comparison. The admittance amplitude and the resonant frequencies in Figs. 3 and 4 are the same order of magnitude. It is also found in calculation that the error between the theoretical values and the experimental values becomes significant only in high-frequency range beyond 2800 Hz. It is well recognized that resonant frequencies of cracked structures decrease with cracks because of the reduction of the local rigidity. From the point of energy, the decrease of the peak values of admittance shows the energy consumption of the longitudinal wave, which reflects energy requirement in the piezoelectric system. A maximum error of 1.92% is found at the fifth mode frequency as crack depth ratio is 0.6125 in Table 1, which shows that the calculated results agree well with the experimental values.

Next, the present theoretical model will be further validated for different boundary conditions and different crack types. A simple-supported aluminum beam with one single-edge crack and a simple-supported steel beam with a double-edges crack beam are chosen as the second numerical example, since the two cracked

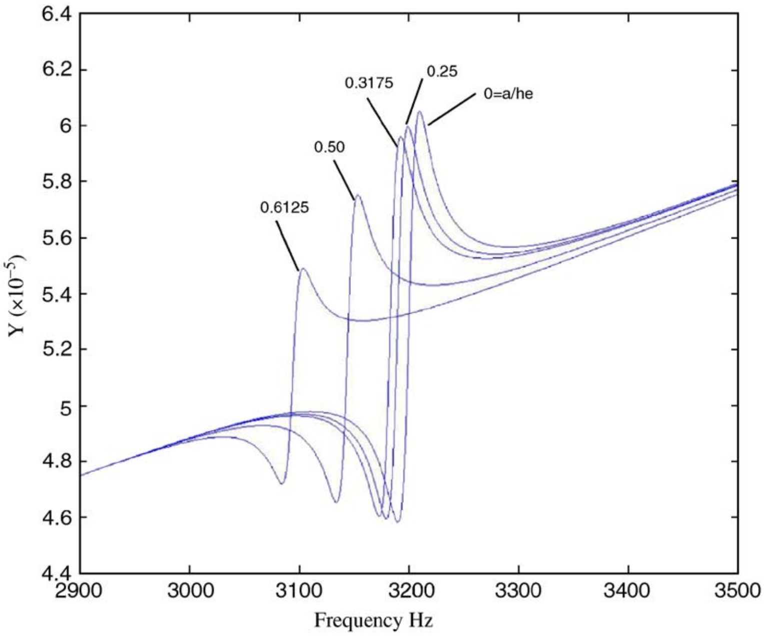

Fig. 3. The calculated admittance curves.

Table 1
Comparison of system frequencies (Hz) for different crack depth ratio a/h_e

Mode number	$a/h_e = 0$		$a/h_e = 0.375$		$a/h_e = 0.6125$	
	Experimental	Calculated	Experimental	Calculated	Experimental	Calculated
Second	178.6	179.5	176.4	177.8	172.1	167.6
Third	350.1	351.6	349.4	351.5	348.5	350.7
Forth	579.3	584.5	568.0	572.0	557.6	542.5
Firth	887.0	877.8	882.9	874.5	878.0	861.1
Sixth	1215.0	1214.0	1204.3	1209.3	1195.2	1185.8
Seventh	1613.0	1619.7	1591.2	1613.6	1557.5	1537.4

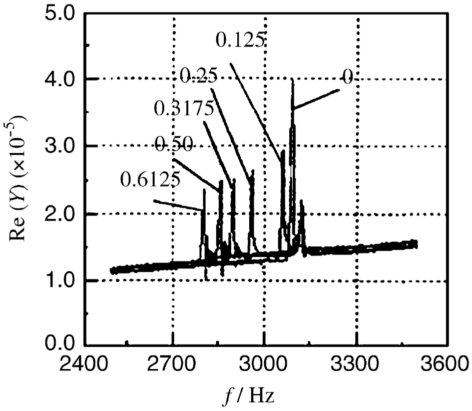

Fig. 4. The experimental admittance curves.

beams without piezoelectric elements are experimentally studied before [7,10]. A crack is located at the midspan of the two beams. The material properties and dimensions of the two beams are:

$$\rho_e = 2800\,\mathrm{kg/m^3},\ v = 0.35,\ E_e = 7.2\times10^{10}\,\mathrm{N/m^2},\ h_e = 0.0254\,\mathrm{m},\ w_e = 0.006\,\mathrm{m},\ L = 0.235\,\mathrm{m}$$

for the aluminum beam [10] and

$$\rho_e = 7800\,\mathrm{kg/m^3},\ v = 0.35,\ E_e = 2.06\times10^{11}\,\mathrm{N/m^2},\ h_e = 0.03175\,\mathrm{m},\ w_e = 0.00952\,\mathrm{m},\ L = 0.575\,\mathrm{m}$$

for the steel beam [7].

In order to verify the present model, a pair of active piezoelectric elements is assumed to be bonded to the above two beams to sense the crack. The piezoelectric material PZT-G1195 is used, whose material properties, dimensions and relative locations to the beams are:

$$\rho_p = 7650\,\mathrm{kg/m^3},\ v = 0.31,\ E_p = 6.3\times10^{10}\,\mathrm{N/m^2},\ d_{31} = -1.66\times10^{-14}\,\mathrm{m/V},$$
$$u_{33}^{\sigma} = 1.5\times10^{-8}\,\mathrm{F/m},\ h_p = 0.0005\,\mathrm{m}.$$
$$w_p = 0.006\,\mathrm{mm},\ L_1 = 0.04\,\mathrm{m},\ L_p = 0.02\,\mathrm{m}\ \text{for the single-edge cracked beam, and}$$
$$w_p = 0.00952,\ L_1 = 0.1\,\mathrm{m},\ L_p = 0.04\,\mathrm{m}\ \text{for the double-edges cracked beam.}$$

It can be seen from the above data that the mass and stiffness of the piezoelectric elements are small enough to be ignored, comparing with those of the beam. It is assumed that the applied AC to the piezoelectric actuators is 5 V which is applied by the impedance analyzer.

The frequencies changes with different crack depth ratios are calculated and shown in Fig. 5 for the single-edge cracked beam and in Fig. 6 for the double-edges cracked beam. The frequencies results of the cracked beam obtained by other methods, sourcing from Refs. [7,10] are respectively copied in Figs. 5 and 6 for comparison, but there are no piezoelectric elements in Refs. [7,10].

It can be seen from Figs. 5 and 6 that a good agreement is achieved among these results, even though the piezoelectric elements are not used in these researches about cracked beams [7,10]. This conclusion is quiet reasonable, because the mass and stiffness of the piezoelectric elements are far smaller than that of the host structure, which has been mentioned above. It is also found in calculations that the crack at midspan has little effect on the even-order mode frequencies of the two beams. These characteristics can be used to detect the crack location, provided that the frequencies covering the multiple modes can be sensed by active piezoelectric elements.

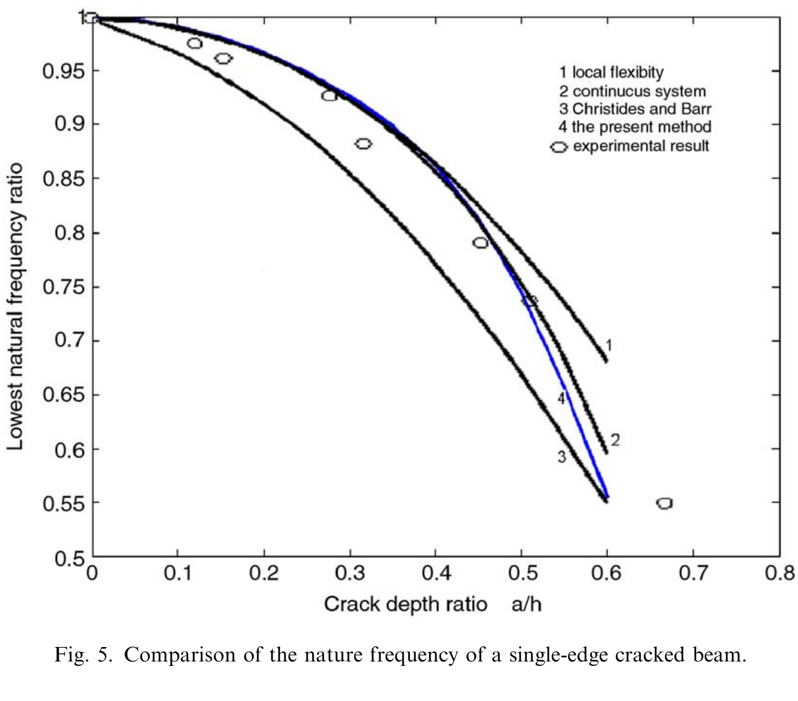

Fig. 5. Comparison of the nature frequency of a single-edge cracked beam.

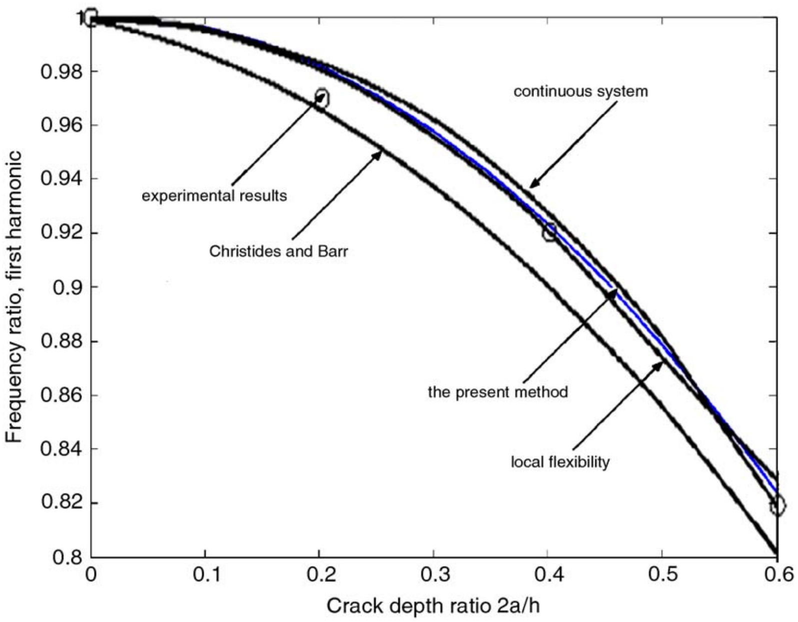

Fig. 6. Comparison of the nature frequency of a double-edges cracked beam.

5. Conclusive remarks

A cracked beam with a pair of piezoelectric patches which are symmetrically bonded on the beam is extensively studied in this paper. The electric admittance function of the system is built by solving linear impedance equations, and the changes of the admittance amplitude and the resonant frequencies of the cracked beam are obtained.

Simply supported or free–free beams with single-edge or double-edges cracks actuated by piezoelectric elements are widely studied. The resonant frequencies of cracked beams are obtained from the admittance function and compared with the results obtained by experiments and other methods. Good agreements are achieved among these results. The changes of the peak values and corresponding frequencies of admittance curves are consistent with the measured curves. The resonant frequencies of cracked beams, which can be extracted from admittance curves, decrease with increase of crack depth. Crack at different locations has distinct influence on the even-mode and odd-mode vibration of the cracked beam. Hence, the active elements can be used to detect the crack, provided that the piezoelectric actuators are bonded at an opportune position on the beam.

References

[1] R.D. Adams, P. Cawley, C.J. Pye, B.J. Stone, A vibration technique of non-destructive assessing the integrity of structure, *Journal of Mechanical Engineering Science* 20 (1987) 93–100.

[2] F.D. Ju, M. Akgun, T.L. Paez, E.T. Wang, *Diagnosis of fracture damage in simple structure*. Bureau of Engineering Research, Report No. CE-62(82) AFOSR-993-1, University of New Mexic, Alburqueque, NM.

[3] Y. Narkis, Identification of crack location vibrating simply supported beams, *Journal of Sound and Vibration* 172 (1994) 549–588.

[4] H.P. Lee, T.Y. Ng, Natural frequencies and modes for the flexural vibration of a cracked beam, *Applied Acoustic* 43 (1995) 151–163.

[5] G. Bamnipos, A. Trochides, Dynamic behavior of a cracked cantilever beam, *Applied Acoustic* 45 (1995) 97–112.

[6] M. Boltezer, B. Strancar, A. Kuhelj, Identification of transverse crack location in flexural vibrations free–free beam, *Journal of Sound and Vibration* 211 (1998) 729–734.

[7] S. Christides, A.D.S. Barr, One-dimensional theory of cracked Bernoulli–Euler beams, *International Journal Mechanics Science* 26 (1984) 639–648.

[8] M.H.H. Shen, C. Pierre, Natural modes of Bernouilli–Euler beams with symmetric cracks, *Journal of Sound and Vibration* 138 (1990) 115–134.

[9] J. Fernandez-Saez, L. Rubio, C. Navarro, Approximate calculation of the fundamental frequency for bending vibrations of cracked beam, *Journal of Sound and Vibration* 225 (1999) 345–352.
[10] T.G. Chondros, A.D. Dimarogonas, J. Yao, A continuous cracked beam vibration theory, *Journal of Sound and Vibration* 215 (1998) 17–34.
[11] M. Chati, R. Rand, S. Mukerjee, Model analysis of a cracked beam, *Journal of Sound and Vibration* 227 (1997) 249–270.
[12] S.L. Tsyfansky, V.T. Beresnevich, Detection of fatigue cracks in flexural geometrically non-linear bars by vibration monitoring, *Journal of Sound and Vibration* 213 (1998) 159–168.
[13] T.G. Chondros, A.D. Dimarogonas, J. Yao, Vibration of a beam with a breathing crack, *Journal of Sound and Vibration* 239 (2001) 57–67.
[14] E.F. Crawley, J. Deluis, Use of piezoelectric actuators as elements of intelligent structures, *AIAA Journal* 25 (1987) 1373–1385.
[15] G.S. Aqnes, Development of a modal model for simultaneous active and passive piezoelectric vibration suppression, *Journal of Intelligent Material Systems and Structures* 6 (1995) 482–487.
[16] C. Liang, F. Sun, C.A. Rogers, Couple electric–mechanical analysis of adaptive material systems-determination of the actuator power consumption and system energy transfer, *Journal of Intelligent Material Systems and Structures* 8 (1997) 335–344.
[17] Y.S. Cho, Y. Eugene Pak, C.S. Han, S.K. Ha, Five-port equivalent electric circuit of piezoelectric bimorph beam, *Sensors and Actuators* 84 (2000) 140–148.
[18] K.E. Castanien, C. Liang, Application of active structural health monitoring technique to aircraft fuselage structures, *Proceedings of SPIE* 2721 (1996) 38–49.
[19] V Lopes Jr., G. Park, H.H. Cudney, D.J. Inman, Impedance-based structural health monitoring with artificial neural networks, *Journal of Intelligent Material Systems and Structures* 11 (2000) 206–214.
[20] G. Pak, H.H. Cudney, D.J. Inman, Feasibility of using impedance-based damage assessment for pipeline structures, *Earthquake Engineering and Structural Dynamics* 30 (2001) 1463–1474.
[21] G. Feng, L. Yi-Nong, W. De-Jun, Research on piezoelectric impedance technology for structure health monitoring, *Journal of Vibration Engineering* 13 (2000) 94–99 (in Chinese).
[22] G. Feng, S. Ya-Peng, Detection of structural crack based on piezoelectric admittance method, *Journal of Experimental Mechanics* 15 (2000) 60–67 (in Chinese).
[23] A.S.K. Naidu, C.K. Soh, Damage severity and propagation characterization with admittance signatures of piezo transducers, *Smart Materials and Structures* 13 (2004) 393–403.
[24] S. Chinchalkar, Determination of crack location in beams using natural frequencies, *Journal of Sound and Vibration* 247 (2001) 417–429.
[25] J.-M. Kim, N. Stubbs, Crack detection in beam-type structures using frequency date, *Journal of Sound and Vibration* 259 (2003) 145–160.
[26] S.A. Paipetis, A.D. Dimarogonas, *Analytical Methods in Rotor Dynamic*, Elsevier Applied Science, London, 1986.